ENCIT 2018

ABCM Associação Brasileira de Engenharia e Ciências Mecânicas

17th Brazilian Congress of Thermal Sciences and Engineering
November 25th-28th, 2018, Águas de Lindóia, SP, Brazil

# ENCIT-2018-0513
# IMPLEMENTATION OF THE FLAMELET-GENERATED-MANIFOLD FOR PREMIXED LAMINAR FLAMES WITH HEAT LOSS

**Leonardo Sebem Donatti**
**André Carlos Contini**
**Cristian Alex Hoerlle**
**Leonardo Zimmer**
**Lisandro Maders**
**Fernando Marcelo Pereira**
Federal University of Rio Grande do Sul, Department of Mechanical Engineering, Porto Alegre, Brazil
leonardo.donatti@ufrgs.br
andre.contini@ufrgs.br

***Abstract.*** *It is still a challenging task to numerically solve flames using detailed chemical kinetics in multidimensional geometries of practical applications. To overcome this difficulty, many efforts have been done to develop chemical kinetics reducing techniques, such as ILDM, FPV, FPI and FGM. Although these techniques are widely discussed in the literature, their implementation are not straightforward. In the present work the FGM technique is implemented in a two-dimensional laminar premixed flame of* $CH_4/air$ *with heat losses. The temperature,* $CO$ *mass fraction and burning velocity along the flame surface are presented and limitations of the technique were identified by comparing FGM results against the direct integration of the full set of conservation equation. In general, the FGM technique has shown a good agreement when compared with direct integration.*
***Keywords:*** *FGM, heat loss, laminar premixed flame.*

## 1. INTRODUCTION

Many efforts have been made worldwide to reduce the fossil fuels consumption, even so, they will remain as the main energy source for the next decades (IEA, 2017). In Brazil, where the production of renewable energy is significantly higher compared with other countries, the energy from fossil fuel represented $52.5\%$ of the energy matrix in 2016 (EPE, 2017). These numbers lead to the development of new technologies and studies to enhance the combustion process efficiency.

Combustion presents a strong coupling with high non-linear dependence among chemical, fluid dynamic, thermodynamics and heat transfer processes. Thus, modeling flames in practical industrial applications using detailed reaction mechanisms are still prohibitive due to the high CPU-time required to solve a large number of species and reactions. In this is way there is a long-standing interest to develop reliable combustion models with high accuracy at low computation time. Chemical reduction techniques intend to meet these requirements for numerical simulations of flames. One alternative is to conduct automatic reduction of chemical mechanisms assuming steady-state and partial equilibrium (Peters, 1985; Peters and Rogg, 1993).

Other reduction methods assume that the flow time scale is much higher than the chemical time scales, hence flow and chemistry can be decoupled. Two of the most popular applications of this assumption is the Intrinsic Low-Dimensional Manifold (ILDM) developed by Maas and Pope (1992) and the steady laminar flamelet model developed by Peters (1984). However, the former is pointed out to lose accuracy in colder regions of the flame (van Oijen, 2002) while the later does not have the ability to describe ignition or extinction processes.

Thereby, van Oijen (2002) proposed the Flamelet-Generated Model (FGM) technique to overcome these problems. In the FGM framework, a database representing the combustion process is built from storing a set of laminar one-dimensional flames solved with detailed chemical kinetic (*flamelets*) as function of some control variables. In some cases, this methodology can be a hundred times faster than the direct integration of the conservation equation (van Oijen, 2002; Donini *et al.*, 2015b) without losing much accuracy. Similar approaches as the FGM are Flamelet/Progress Variable Model (FPV) proposed by Pierce and Moin (2004) and the Flame Prolongation ILDM (FPI) proposed by Fiorina *et al.* (2003).

The solution of premixed flame with heat loss using the FGM technique has been initially studied by van Oijen *et al.* (2001). The authors have explored a 2D laminar premixed flame and validated their results with a detailed model. Then, the authors explored their model in a radiating furnace with a ceramic-foam surface burner on the upper wall. The numerical simulation using FGM agreed well with experimental measurements. Donini (2014) has presented numerical results for the DLR burner with heat loss at the walls using the FGM technique. In his work, a preliminary study considering a flame in a box (2D geometry) is carried out to test the heat loss implementation. Fancello (2014) also develop a preliminary study using a 2D geometry with heat loss before exploring a 3D geometry.

In the present work, the heat loss in the FGM technique is also implemented and validated by comparing against the direct integration of the full set of conservation equation. The case of study is a flame in a box similar to those studied by van Oijen *et al.* (2001). The results of temperature, mass fraction of $CO$, and the prediction of the burning velocity distribution along the flame surface are presented and discussed in detail.

## 2. PROBLEM DEFINITION

The problem studied (presented in Fig. 1) is a two-dimensional box. The inlet is 4 $mm$ wide and the outlet 12 $mm$ wide. The walls and the gas inlet are maintained at a constant temperature equals to 298 $K$. The fresh gas velocity has a parabolic profile with a maximum value of 1.1 $m/s$. The outlet surface is assumed to be at 1 atm. The problem is the same test case already described by Somers and De Goey (1995) and Fiorina *et al.* (2003).

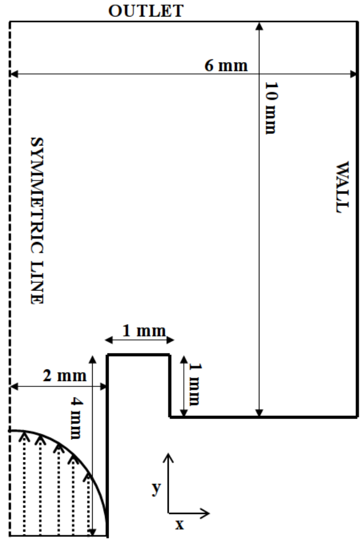


Figure 1: 2D Burner configuration.

## 3. THE FGM METHOD

Flamelets solutions, at a specific equivalence ratio, are obtained for different levels of heat losses, and then, stored in a database (a manifold) as a function of some control variables. After the manifold construction, multidimensional simulations are conducted solving only the conservation of total mass, momentum and transport equations for the control variables. Conservation equations of each chemical species are not required as in detailed simulations. Once the convergence is achieved, the multidimensional structure of the flame is reconstructed from the manifold with the control variables solution. The flamelet equations, the appropriate definition of control variables, and the manifold generation are described in the next sections.

### 3.1 Manifold construction

The initial step of the FGM methodology is to solve a set of one-dimensional flames to map the thermo-chemical space. The method to account for the enthalpy changes on the flames will be clearly described in the next subsection. First, the system of conservation equations describing detailed laminar freely propagating premixed flames is solved through the one-dimensional laminar flame code Chem1D (van Oijen, 2002; Chem1D, n.d.). The equation system accounts for conservation of total mass, chemical species mass fraction and mixture specific enthalpy. The conservation equations - neglecting curvature, stretch, and tangential diffusion - are solved for the steady-state regime. The boundary conditions are presented in the Table 1.

Flames are computed with the DRM22 kinetic mechanism (formed by 22 species and 104 reactions) (Kazakov and Frenklach, 1995). Transport properties are simplified by the unity Lewis number assumption. A diffusion velocity correction is considered for $N_2$ to ensure the total mass conservation. Mixture thermal conductivity and dynamic viscosity are obtained from simplified polynomial expressions as function of mixture specific heat and temperature following Smooke

| Unburnt Side ($Left$) | Burnt Side ($Right$) |
|---|---|
| $Y_i(-\infty) = Y_i$ | $\partial Y_i/\partial s(+\infty) = 0$ |
| $h(-\infty) = h$ | $\partial h/\partial s(+\infty) = 0$ |

Table 1: Boundaries condition imposed to solve a free flame.

and Giovangigli (1991). Species specific heat is obtained according to (McBride *et al.*, 1993; Burcat and C. Gardiner Jr, 2000). It was found that a computational domain of 2.5 cm discretized in 100 volumes was sufficient to achieve mesh independent solutions.

In the next step, any scalar $\psi$ from the flamelet solutions are tabulated as function of the control variables. For non-adiabatic laminar premixed flames at constant pressure, at least two control variables are required to predict the general flame structure (Donini, 2014; van Oijen, 2002). The control variables, in this case, are the progress variable ($\mathcal{Y}$) and enthalpy ($h$). The two control variables form a 2D manifold where $\psi = \psi(\mathcal{Y}, h)$. The progress variable describes the chemistry evolution from unburnt reactants to combustions products. According to van Oijen (2002), a progress variable could be represented by a linear combination of any species mass fraction, $Y_i$. However, determining an excellent definition progress variable is not an easy task and it is usually assumed to be a combination of major combustion products. The enthalpy maps different thermodynamic states due to heat losses to the burner walls and to the environment. For more complex combustion problems, for example, an increased number of control variables would be required for a better description of the process (Donini *et al.*, 2015a), but with penalty in the CPU-time. In addition, control variables are conserved scalars that must uniquely describe each position in the thermo-chemical space, so that flamelets solution must be monotonic in respect to $\mathcal{Y}$ (i.e., for each enthalpy level $\nabla\mathcal{Y} > 0$ should be respected). In this work it was sought from literature the $\mathcal{Y}$ definition used by Donini (2014):

$$\mathcal{Y} = -\alpha_{O_2}Y_{O_2} + \alpha_{CH_4}Y_{CH_4} + \alpha_{H_2O}Y_{H_2O} + \alpha_{H_2}Y_{H_2} \tag{1}$$

where the weighting factor ($\alpha_i$) is given by the inverse of the species $i$ molecular mass ($\alpha_i = 1/MW_i$). Finally, the full set of flamelet solutions are linearly interpolated into the manifold as a function of the control variables. The final manifold is discretized in 200 points in the $\mathcal{Y}$ direction and 70 points in the $h$ direction, with all points being equally spaced. The reader is referred to van Oijen and de Goey (2000) for more details about the stored procedure.

#### 3.1.1 Inclusion of heat losses in the manifold

For predicting heat losses, the flamelets were solved for a range of enthalpies values, which implies that enthalpy becomes a control variable. The easiest way to change the mixture enthalpy is by changing the inlet boundary initial temperature. Thus, in the present work, the flamelets were calculated for initial temperatures varying from 390 K to 240 K in steps of 30 K (following van Oijen (2002)). Thus, the manifold includes conditions of heat gain (initial temperature bigger than 298 K) and heat loss (initial temperature smaller than 298 K). Computing flamelets for even lower temperatures may become unrealistic. In the literature, there are a couple of ways to solve this problem (van Oijen, 2002; Donini, 2014). In this paper, we follow the approach of converting part of the reactants into the corresponding products.

In the present work, we followed the approach of converting a fraction of the reactants ($CH_4$ and $O_2$) into the corresponding products ($CO_2$ and $H_2O$) at the same initial temperature. This conversion of species respects the fuel/oxidant stoichiometric proportion, thus, the enthalpy of the mixture is decreased, due to the low enthalpy of formation of the saturated products, while the pool of atoms of the mixture is preserved. Hence, we changed the composition, increasing the molar fraction of $CO_2$ ($H_2O$) in steps of 0.01 (0.02) until the flame extinguishes.

The enthalpy range covered by the decrease of the initial temperature and the dilution of the reactants with products is shown in Figure 2. Unfortunately, these two methods are not able to reproduce the cold states close to the walls, where reactions are negligible. For this region an extrapolation procedure is necessary (van Oijen, 2002). Here the lowest enthalpy composition is approximated for the one obtained from equilibrium calculations at 298K and imposing the initial composition equal to that obtained for the last flamelet solution for the maximum progress variable (Figure 2).

### 3.2 Multi-dimensional simulations

FGM simulations in multi-dimensional geometries are ready to be executed once the database (manifold) is constructed. These simulations consist in solving laminar steady-state conservation equations of total mass, momentum and a conservation equation for each control variables. Assuming unity Lewis number, the transport equation for $\mathcal{Y}$ and $h$ are given by:

$$\nabla \cdot (\rho\vec{u}\mathcal{Y}) - \nabla \cdot (\frac{\lambda}{c_p}\nabla\mathcal{Y}) = \dot{\omega}_{\mathcal{Y}} \tag{2}$$

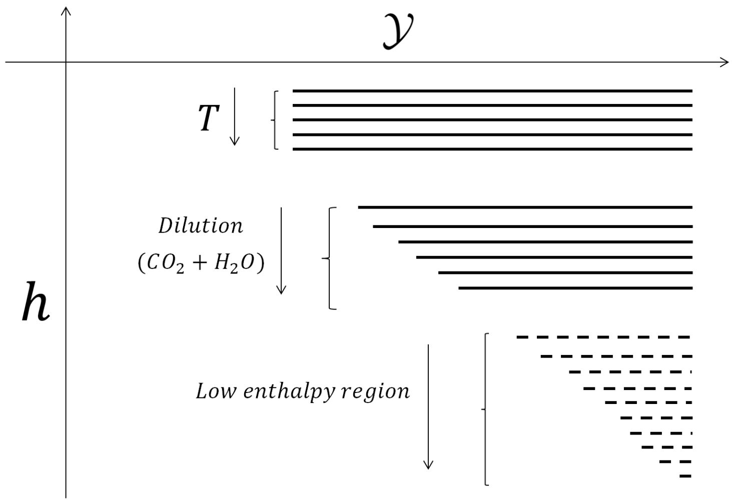


Figure 2: Schematic representation of 2D manifold with the different approaches for distinct regions.

$$\nabla \cdot (\rho \vec{u} h) - \nabla \cdot (\frac{\lambda}{c_p} \nabla h) = 0 \tag{3}$$

where $\lambda\,[W/mK]$ and $c_p\,[J/kgK]$ is the thermal conductivity and specific heat, respectively. The $\dot{\omega}_{\mathcal{Y}}$ is source term of progress variable, $\vec{u}\,[m/s]$ is the velocity vector and $\rho\,[kg/m^3]$ is defined as the density. The boundaries conditions are presented in the table 2.

| Boundaries | $\mathcal{Y}$ | $h$ |
|---|---|---|
| Inlet | min($\mathcal{Y}$) | $h(T = 298\,K)$ |
| Outlet | $\frac{\partial \mathcal{Y}}{\partial x_i} = 0$ | $\frac{\partial h}{\partial x_i} = 0$ |
| Walls | $\frac{\partial \mathcal{Y}}{\partial x_i} = 0$ | $h(T = 298\,K)$ |

Table 2: Boundaries condition imposed for $\mathcal{Y}$ and $h$ transport equations.

The equation system for multidimensional simulations is solved by the Fluent 16.1 software. The FGM technique is implemented in the software via user-defined functions (UDFs), including the conservation equations for the control variables and the retrieval procedure of information from the manifold. Mixture thermodynamic and transport properties (as viscosity conductivity and specific heat) required for the solution of the equation system are retrieved from the manifold during run-time. After the solution of the equation system, the flame structure is reconstructed from the solution of control variables retrieving the temperature and the species mass fractions from the manifold. The look-up/retrieval scheme is based on bilinear interpolations van Oijen (2002) between the closest values of $\mathcal{Y}$ and $h$ solution at each volume of the mesh. Additionally, in Fluent simulations the pressure-velocity coupling is treated by the SIMPLE method, the convective and diffusive terms are discretized by second-order schemes and a residual error of $10^{-6}$ is assumed as convergence criterion.

### 3.2.1 Mesh independence test

A mesh independence test for the 2D domain is performed using the FGM technique. The computational domain is discretized with equally sized quadrilateral cells. The analysis is conducted for six different meshes from 260 to 650000 volumes. Flame temperature is chosen as the parameter to evaluate the mesh independence. Figure 3a exhibits the temperature profile at 7 mm from the nozzle exit. Maximum discrepancies are observed at 4.5 mm from the symmetry line. Therefore, Fig. 3b presents the temperature relative error in respect to the most refined mesh at 4.5 mm from the symmetry line and 7 mm from the nozzle exit. It is observed that the relative error is less than 2.5% for the mesh formed by 6500 volume, hence, this discretization is applied for subsequent two-dimensional simulations.

## 4. DETERMINATION OF LAMINAR BURNING VELOCITY FROM THE TWO DIMENSIONAL FLAMES

The two-dimensional flame analyzed in the present work is more complex than the idealized one-dimensional canonical planar adiabatic flame. It has been shown that stretch and curvature effects may significantly change the burning velocity (Law, 2006). Additionally, heat losses reduce the flame temperature, which has an exponential effect on the

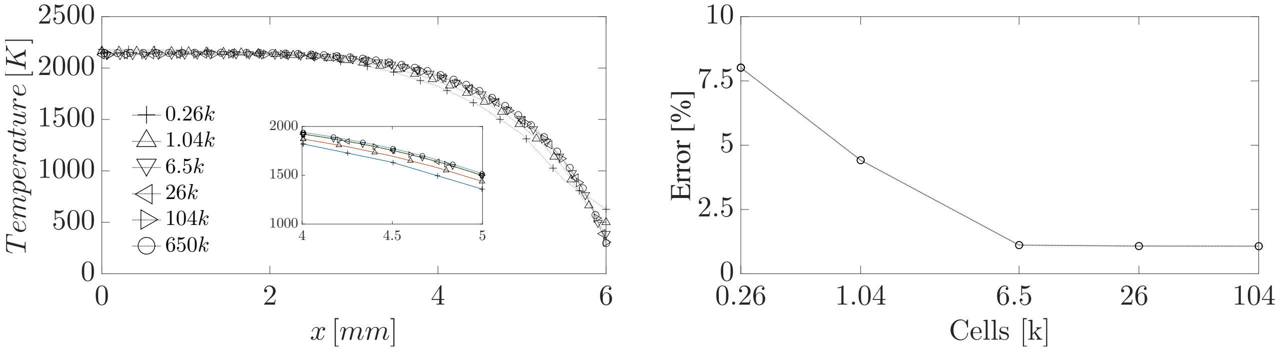


(a) (b)

Figure 3: Mesh independence test: (a) temperature profile for different meshes at 7 mm from the burner nozzle exit; (b) relative error at 4.5 mm from symmetry line and 7 mm from the nozzle exit.

reaction rates and, consequently, on the burning velocity (Law, 2006). In this work, the laminar burning velocity along the flame surface are extracted in order to compare FGM and detailed solutions. Both results are compared with the one-dimensional standard calculation and the observed behavior is discussed.

The laminar burning velocity,$S_l$, is defined at the unburnt region of the flame (cold boundary). In the two-dimensional results this region is approximated by an isothermal surface with a temperature equal to $315K$ (which represents a variation of, approximately, 1% of the adiabatic temperature). Points on this isothermal surface are collected by following the temperature evolution along a certain number of streamlines as shown in Fig. 4. Then, the points are used to reconstruct the surface by a polynomial fit. At this surface, the flow velocity is determined and its projection on the normal surface direction is obtained. This velocity projection is equal to the laminar burning velocity $S_l$.

In order to reveal the heat loss effects, a similar procedure is developed for the flame temperature. In this case, the position of the maximum heat release rate is found for each streamline and the flame temperature is collected at this position. Note that this temperature is not the maximum value reached by the flame, instead it is a temperature that characterizes the inner structure of the flame, where most reactions are happening.

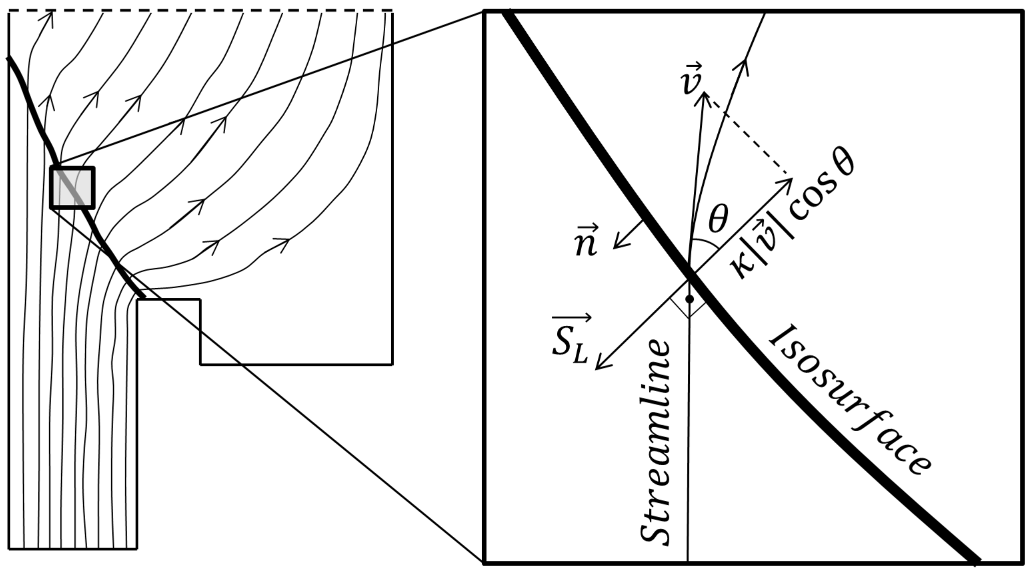


Figure 4: Extraction of the burning velocity from the two-dimensional results ($\kappa$ value is the ratio between $298/315$).

## 5. RESULTS

### 5.1 Manifold validation

Figure 5 shows the validation of the present implementation in a 1D configuration, considering a freely propagating flame of $CH_4/Air$ with stoichiometric equivalence ratio. The inlet temperature of the mixture is 298 K and atmospheric pressure is imposed. The results present discrepancies of order of the 1% for both temperature and $CO$ mass fraction when they are compared with the detailed simulation. This result suggests that the FGM technique can correctly solve the flame and that the progress variable is suitable to solve the problem.

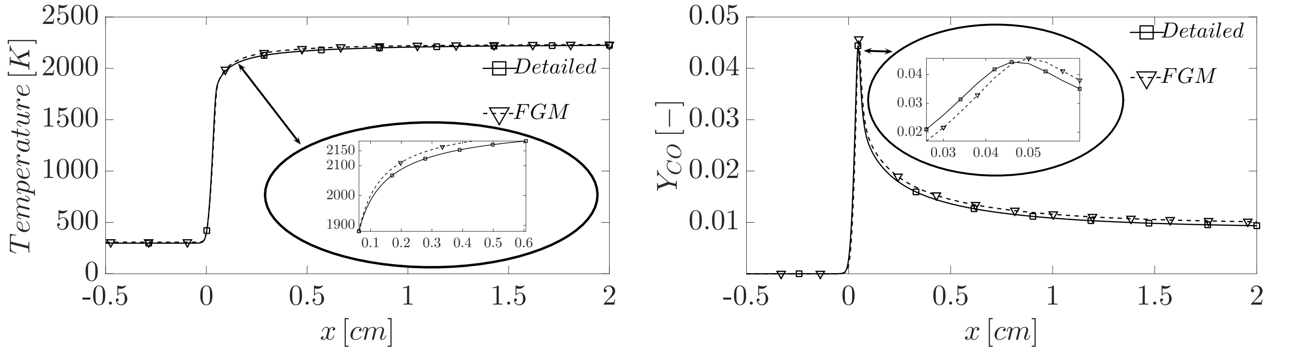


(a) (b)

Figure 5: Manifold validation for one-dimensional adiabatic freely propagating flame of $CH_4/Air$ at $\phi = 1.0$ and atmospheric conditions. Comparison of FGM and detailed model for (a) temperature and (b) $CO$ mass fraction.

### 5.2 Bi-dimensional simulations

Bi-dimensional simulations were conducted for the configuration presented in Fig. 1 following the FGM methodology explained in Section 3.

#### 5.2.1 Comparison of FGM and detailed simulations

FGM and detailed results are compared for profiles of temperature and $CO$ mass fraction at 1 mm, 3 mm and 7 mm from the burner nozzle exit. These positions approximately indicate the bottom and the middle of the flame, and the post-flame region. Figure 6 presents temperature profiles computed with detailed simulations and the FGM method. A negligible displacement of FGM results is observed at the regions with higher gradients. A good quantitative and qualitative agreement is also observed for the major chemical species. For, example, Fig. 7 shows the $CO$ mass fraction at the three axial positions.

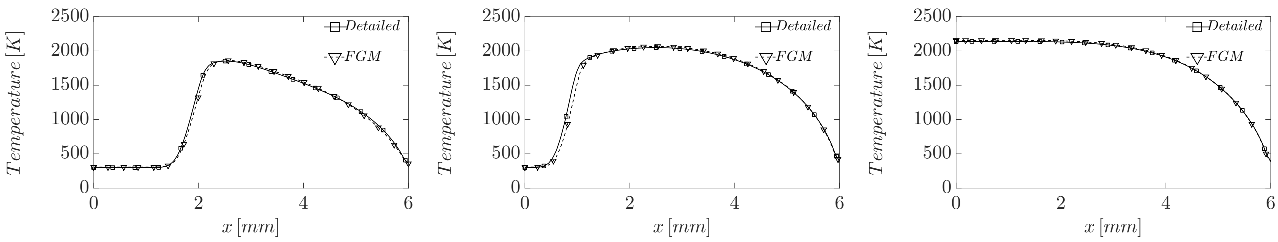


(a) (b) (c)

Figure 6: Comparison of temperature profiles between detailed and FGM simulations at (a) 1 mm, (b) 3 mm and (c) 7 mm from the burner nozzle exit.

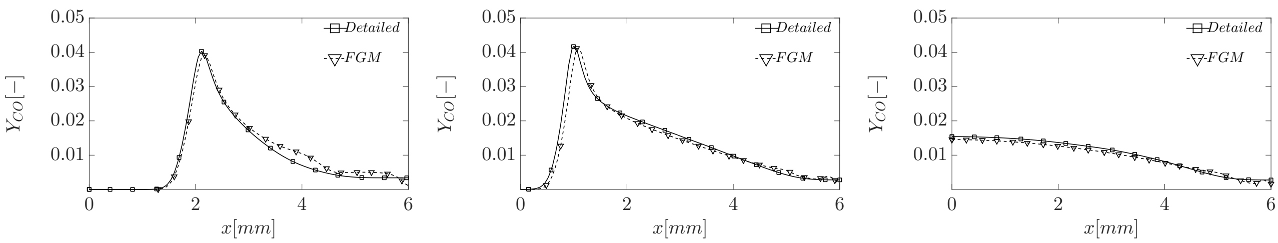


(a) (b) (c)

Figure 7: Comparison of $CO$ mass fraction profiles between Detailed and FGM simulations at (a) 1 mm, (b) 3 mm and (c) 7 mm from the burner nozzle exit.

Contours of $CO$ mass fraction are presented in Figure 8a. We can observe a small difference that occurs next to the burner rim where the flame stabilizes. It is the region where the flame extinguishes due to low the temperatures next to the wall. In this region, the reactants can leak through the flame envelope without being completely burnt. As discussed in Donini (2014), this effect could be captured by the FGM method extending it with an extra control variable which keeps track of $CO$. Possible implementation problems of the low enthalpy region of the manifold are still under investigation. Another difference between the solutions is observed at the flame tip (Fig. 8b). The smaller flame hight suggests that the laminar flame speed is slightly under-predicted by the FGM technique. To better capture this effects, a possibility would be to consider the stretch and the curvature effects in an additional control variable. Despite these discrepancies, the results achieved with the FGM approach presented a good agreement with the detailed simulations demanding only a fraction of the computational time. While detailed simulation required roughly 48 hours to converge, the FGM methodology needed only 2.4 hours (20 times faster), including the pre-processing step (flamelet simulations and manifold construction). Also, it should be noted that the manifold needs to be created just once for each thermo-chemical space under consideration. In other words, the same manifold can be used to perform simulations of different burners subjected to different heat loss conditions.

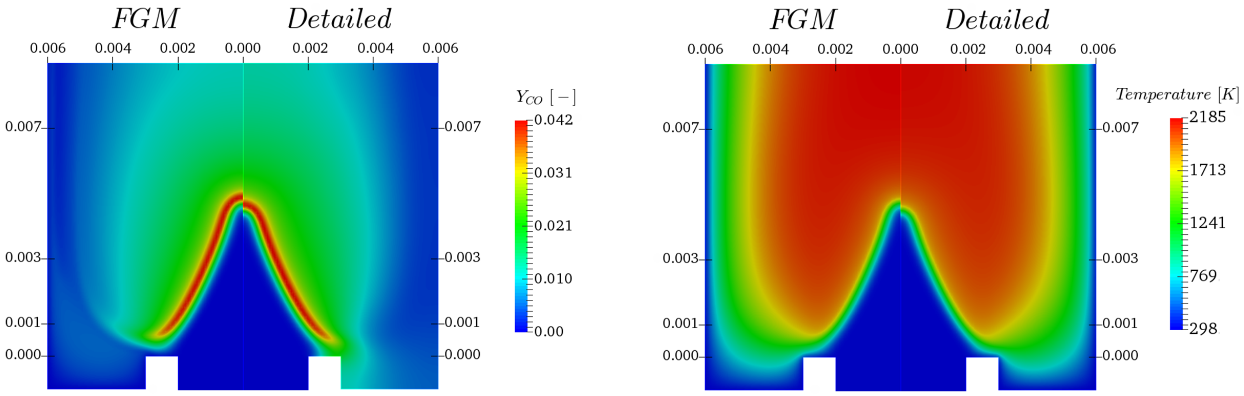


(a) (b)

Figure 8: Contours of (a) CO mass fraction and (b) temperature, both computed with the FGM technique and the detailed simulation.

### 5.3 Flame structure and laminar flame speed

Figure 9a shows the burning velocity along the flame surface (the coordinate $x$ is the horizontal axis). Three distinct regions are observed: one close to the burner rim, which is affected by heat losses, an intermediary region, which approaches the 1D results and a third region close to the centerline, where the flame is affected by curvature effects. The FGM and the detailed results are very similar showing, again, the good approximation obtained with the reduced technique.

Figure 9b shows that as the distance increases, the temperature at the reaction region is reduced due to heat losses to the burner rim. This explains why there is a decrease of the burning velocity in this region. In the second region, $S_l$ is almost constant, with a value next to the $S_l^o$. This region represents a reasonable approximation of the 1D results because heat losses and curvature effects are low. Finally, in the region close to the symmetry axis we see an intense increase of the burning velocity. This effect can be understood by the analysis proposed by Law (2006):

$$\frac{S_l}{S_l^o} = 1 - \delta_u^o \nabla \cdot n \tag{4}$$

were $\delta_u^o$ is the flame thickness and $\nabla \cdot n$ represents the flame curvature (which is equal to $-2/R_f$, were $R_f$ is the surface radius). Thus, the burning velocity is increased at the tip of the conical flame due to pure curvature effects. Note that since in our simulations we are considering unitary Lewis number, stretch effects are not present.

The burning velocities predicted by the FGM technique are slightly lower than those obtained with the detailed model. This result helps explaining why in Fig. 8 the contours for temperature and CO mass fraction obtained with FGM are displaced upwards relative to the detailed results. Due to the lower burning velocities the FGM flame reaches an equilibrium with the flow slightly downstream.

In Fig. 9b it is possible to see some important differences in the temperature at the maximum heat release rate position predicted by each method. Both solutions present intense oscillations closer to the centerline and a decrease of temperature closer to the burner rim. The temperature decrease is expected near the rim due to the intense heat loss condition to the cold solid wall. Such heat loss is more intense for the detailed simulation probably because the different stabilization position predicted by the FGM model. Closer to the centerline the temperatures are lower than the one-dimensional reference, showing that the 2D simulations deviate from its one-dimensional counterpart.

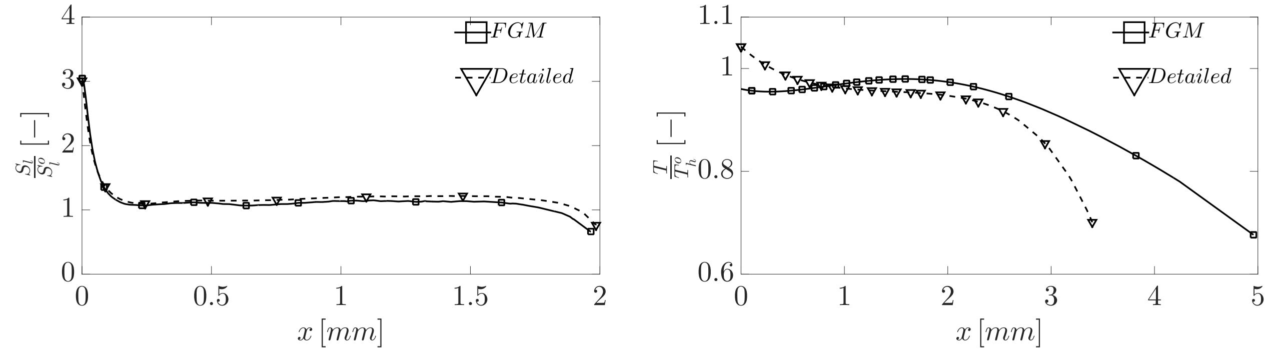


Figure 9: (a) Burning velocity along the flame surface normalized by the 1D burning velocity ($S_l^o$=29.72 $cm/s$) (b) Temperature at the maximum heat release rate position normalized by the same temperature from a 1D adiabatic simulation ($T_h^o$ = 1721 K).

## 6. CONCLUSIONS

In this paper an implementation of the FGM technique for premixed flames with heat losses is compared to the detailed solution of the conservation equations. The problem is a premixed laminar flame stabilized on a slot burner. The FGM technique presented excellent qualitative and very good quantitative results when compared to the reference model. The observed discrepancies are due to the underprediction of the burning velocity for the FGM technique an, possibly, due to the difficulties in mapping the thermochemical state of the system near the walls where the flame extinguishes.

## 7. ACKNOWLEDGEMENTS

The authors kindly acknowledge the financial support of the Petrobras S.A.

## 8. REFERENCES

Burcat, A. and C. Gardiner Jr, W., 2000. *Ideal Gas Thermochemical Data for Combustion and Air Pollution Use*, pp. 489–538.

Chem1D, n.d. *One-dimensional Laminar Flame Code*. Eindhoven University of Technology.

Donini, A., Bastiaans, R., van Oijen, J. and de Goey, L., 2015a. "Differential diffusion effects inclusion with flamelet generated manifold for the modeling of stratified premixed cooled flames". *Proceedings of the Combustion Institute*, Vol. 35, No. 1, pp. 831 – 837. ISSN 1540-7489. doi:10.1016/j.proci.2014.06.050.

Donini, A.A., 2014. *Advanced turbulent combustion modeling for gas turbine application*. Ph.D. thesis, Technische Universiteit Eindhoven.

Donini, A., Bastiaans, R.J., van Oijen, J.A. and de Goey, L.P.H., 2015b. "The implementation of five-dimensional fgm combustion model for the simulation of a gas turbine model combustor". *ASME Paper No. GT2015-42037*.

EPE, 2017. *Brazilian Energy Balance 2016*. Empresa de Pesquisa Energética, Rio de Janeiro.

Fancello, A., 2014. *Dynamic and turbulent premixed combustion using Flamelet-Generated Manifold in OpenFOAM*. Ph.D. thesis, Technische Universiteit Eindhoven.

Fiorina, B., Baron, R., Gicquel, O., Thevenin, D., Carpentier, S., Darabiha, N. *et al.*, 2003. "Modelling non-adiabatic partially premixed flames using flame-prolongation of ildm". *Combustion Theory and Modelling*, Vol. 7, No. 3, pp. 449–470.

IEA, 2017. *Key World Energy Statistics*. International Energy Agency.

Kazakov, A. and Frenklach, M., 1995. "Drm22". *University of California at Berkeley, Berkeley, CA*, Vol. 21, p. 2017.

Law, C., 2006. *Combustion Physics*. Cambridge University Press, 1st edition.

Maas, U. and Pope, S.B., 1992. "Simplifying chemical kinetics: intrinsic low-dimensional manifolds in composition space". *Combustion and flame*, Vol. 88, No. 3, pp. 239–264.

McBride, B.J., Gordon, S. and Reno, M.A., 1993. "Coefficients for calculating thermodynamic and transport properties of individual species".

Peters, N., 1984. "Laminar diffusion flamelet models in non-premixed turbulent combustion". *Progress in Energy and Combustion Science*, Vol. 10, No. 3, pp. 319 – 339. doi:10.1016/0360-1285(84)90114-X.

Peters, N., 1985. "Numerical and asymptotic analysis of systematically reduced reaction schemes for hydrocarbon flames". In *Numerical simulation of combustion phenomena*, Springer, pp. 90–109.

Peters, N. and Rogg, B., 1993. "Reduced kinetic mechanisms for applications in combustion systems". *Lecture Notes in*

*Physics*, Vol. 15.

Pierce, C.D. and Moin, P., 2004. "Progress-variable approach for large-eddy simulation of non-premixed turbulent combustion". *Journal of fluid Mechanics*, Vol. 504, pp. 73–97.

Smooke, M.D. and Giovangigli, V., 1991. "Premixed and nonpremixed test problem results". In *Reduced kinetic mechanisms and asymptotic approximations for methane-air flames*, Springer, pp. 29–47.

Somers, L.M. and De Goey, L., 1995. "A numerical study of a premixed flame on a slit burner". *Combustion science and technology*, Vol. 108, No. 1-3, pp. 121–132.

van Oijen, J.A., 2002. *Flamelet-Generated Manifolds: development and application to premixed laminar flames*. Ph.D. thesis, Eindhoven University of Technology.

van Oijen, J.A. and de Goey, L.P.H., 2000. "Modelling of premixed laminar flames using flamelet-generated manifolds". *Combustion Science and Technology*, Vol. 161, No. 1, pp. 113–137. doi:10.1080/00102200008935814.

van Oijen, J., Lammers, F. and de Goey, L., 2001. "Modeling of complex premixed burner systems by using flamelet-generated manifolds". *Combustion and Flame*, Vol. 127, pp. 2124 – 2134.

## 9. RESPONSIBILITY NOTICE

The author(s) is (are) the only responsible for the printed material included in this paper.